Radiology

Diffusion Tractography of the Entire Left Ventricle by Using Free-breathing Accelerated Simultaneous Multisection Imaging[1]

Choukri Mekkaoui, PhD
Timothy G. Reese, PhD
Marcel P. Jackowski, PhD
Stephen F. Cauley, PhD
Kawin Setsompop, PhD
Himanshu Bhat, PhD
David E. Sosnovik, MD

Purpose: To develop a clinically feasible whole-heart free-breathing diffusion-tensor (DT) magnetic resonance (MR) imaging approach with an imaging time of approximately 15 minutes to enable three-dimensional (3D) tractography.

Materials and Methods: The study was compliant with HIPAA and the institutional review board and required written consent from the participants. DT imaging was performed in seven healthy volunteers and three patients with pulmonary hypertension by using a stimulated echo sequence. Twelve contiguous short-axis sections and six four-chamber sections that covered the entire left ventricle were acquired by using simultaneous multisection (SMS) excitation with a blipped-controlled aliasing in parallel imaging readout. Rate 2 and rate 3 SMS excitation was defined as two and three times accelerated in the section axis, respectively. Breath-hold and free-breathing images with and without SMS acceleration were acquired. Diffusion-encoding directions were acquired sequentially, spatiotemporally registered, and retrospectively selected by using an entropy-based approach. Myofiber helix angle, mean diffusivity, fractional anisotropy, and 3D tractograms were analyzed by using paired *t* tests and analysis of variance.

Results: No significant differences ($P > .63$) were seen between breath-hold rate 3 SMS and free-breathing rate 2 SMS excitation in transmural myofiber helix angle, mean diffusivity (mean ± standard deviation, $[0.89 \pm 0.09] \times 10^{-3}$ mm^2/sec vs $[0.9 \pm 0.09] \times 10^{-3}$ mm^2/sec), or fractional anisotropy (0.43 ± 0.05 vs 0.42 ± 0.06). Three-dimensional tractograms of the left ventricle with no SMS and rate 2 and rate 3 SMS excitation were qualitatively similar.

Conclusion: Free-breathing DT imaging of the entire human heart can be performed in approximately 15 minutes without section gaps by using SMS excitation with a blipped-controlled aliasing in parallel imaging readout, followed by spatiotemporal registration and entropy-based retrospective image selection. This method may lead to clinical translation of whole-heart DT imaging, enabling broad application in patients with cardiac disease.

Online supplemental material is available for this article.

[1] From the Athinoula A. Martinos Center for Biomedical Imaging, Department of Radiology (C.M., T.G.R., S.F.C., K.S., D.E.S.), and Cardiovascular Research Center, Cardiology Division (D.E.S.), Massachusetts General Hospital, Harvard Medical School, 149 13th St, Charlestown, MA 02129; Department of Computer Science, Institute of Mathematics and Statistics, University of São Paulo, São Paulo, Brazil (M.P.J.); and Siemens Healthcare, Charlestown, Mass (H.B.). Received November 25, 2015; revision requested January 11, 2016; revision received June 30; accepted July 14; final version accepted July 28. **Address correspondence to** C.M. (e-mail: *mekkaoui@nmr.mgh.harvard.edu*).

C.M. supported by the National Heart, Lung, and Blood Institute (R56HL125590, R01HL131635). D.E.S. supported by the National Heart, Lung, and Blood Institute (R01HL112831, R01HL093038) and the Athinoula A. Martinos Center for Biomedical Imaging (P41RR14075).

Diffusion-tensor (DT) magnetic resonance (MR) imaging of the heart can be performed in vivo with a dual-gated stimulated echo (STE) sequence (1) or a gated motion-compensated pulsed gradient spin-echo sequence (2). Respiratory motion has been addressed by using breath holds, synchronized breathing, or navigator echoes (1,3,4). When combined with the long repetition time and low signal-to-noise ratio (SNR), both methods are inefficient, leading to long imaging times. Consequently, in most studies, DT imaging involving acquisition of a subset of short-axis sections of the left ventricle (LV) has been performed. With this approach, approximately 25% of the LV is imaged in about 20 minutes (4,5). However, accurate evaluation of focal myocardial alterations that affect the three-dimensional (3D) continuum of the heart requires full anatomic coverage (6–8).

Simultaneous multisection (SMS) excitation with blipped-controlled aliasing in parallel imaging (CAIPI) emerged as a unique echo-planar imaging technique to acquire multiple sections simultaneously while minimizing the SNR penalty typical of other acceleration techniques (9,10). SMS has been used for cardiac DT imaging with breath holding but with limited spatial coverage (11).

In this work, we present an approach to perform free-breathing DT imaging that combines SMS with *(a)* sequential acquisition of all repetitions of each diffusion-encoding direction, increasing the likelihood of achieving the largest number of usable images, and *(b)* spatiotemporal registration followed by retrospective selection of free-breathing diffusion images to prevent the use of navigator echoes and controlled respiration. The purpose of this work was to develop a clinically feasible whole-heart free-breathing DT imaging approach with an imaging time of approximately 15 minutes to enable 3D tractography.

Advances in Knowledge

- Diffusion-tensor (DT) imaging of the entire human heart can be performed in vivo by using simultaneous multisection (SMS) excitation with a blipped-controlled aliasing in parallel imaging readout.
- Acquiring all repetitions of each diffusion-encoding direction sequentially increases the likelihood of achieving the largest number of usable images.
- Spatiotemporal registration, followed by retrospective selection of free-breathing diffusion images, prevents the need for navigator echoes or controlled respiration.
- Free-breathing DT imaging of the entire human heart can be performed without section gaps in approximately 15 minutes, enabling three-dimensional tractography.
- SMS-accelerated free-breathing DT imaging compares favorably to breath-hold DT imaging and can be applied to patients with severe cardiopulmonary disease.

Materials and Methods

H.B. is an employee of Siemens Healthcare. No specific support was provided by Siemens for this study. The authors of the article who are not employees of Siemens had full control over all aspects of this study, including its design, inclusion, analysis, and reporting.

Implications for Patient Care

- The ability to perform free-breathing DT imaging of the entire heart in approximately 15 minutes could facilitate the clinical translation of cardiac DT imaging.
- Free-breathing DT imaging enables the measurement of myocardial structure in patients with severe cardiovascular disease.

Pulse Sequence

DT imaging was performed in seven healthy volunteers and three patients with pulmonary hypertension by using a clinical 3-T MR imaging unit (Skyra; Siemens Healthcare, Erlangen, Germany) equipped with a 45-mT/m gradient system and a 34-element cardiac receive coil. Imaging was performed with an electrocardiographically gated diffusion-encoded STE sequence (Fig 1a) volume selected in the phase-encode axis by using a slab-selective radiofrequency pulse (4). Acquisition parameters were field of view of 360 × 200 mm, resolution of 2.5 × 2.5 mm, section thickness of 8 mm, in-plane generalized autocalibrating partially parallel acquisition rate of 2 (12), echo time of 34 msec, *b* values of 0 and 500 sec/mm^2, 10 diffusion-encoding directions, and eight magnitude averages (repetitions). Twelve short-axis sections were acquired at the systolic sweet spot (160 msec after the R wave) to mitigate strain effects

Published online before print
10.1148/radiol.2016152613 **Content codes:** CA MR

Radiology 2017; 282:850–856

Abbreviations:
CAIPI = controlled aliasing in parallel imaging
DT = diffusion-tensor
ERIS = entropy-based retrospective image selection
FA = fractional anisotropy
HA = myofiber helix angle
LV = left ventricle
SMS = simultaneous multisection
SNR = signal-to-noise ratio
STE = stimulated echo
STR = spatiotemporal registration
3D = three-dimensional

Author contributions:
Guarantors of integrity of entire study, C.M., T.G.R., K.S., D.E.S.; study concepts/study design or data acquisition or data analysis/interpretation, all authors; manuscript drafting or manuscript revision for important intellectual content, all authors; approval of final version of submitted manuscript, all authors; agrees to ensure any questions related to the work are appropriately resolved, all authors; literature research, C.M., T.G.R., M.P.J., D.E.S.; clinical studies, C.M., D.E.S.; experimental studies, all authors; statistical analysis, C.M., M.P.J., D.E.S.; and manuscript editing, C.M., T.G.R., M.P.J., H.B., D.E.S.

Conflicts of interest are listed at the end of this article.

See also the editorial by Axel in this issue.

Figure 1

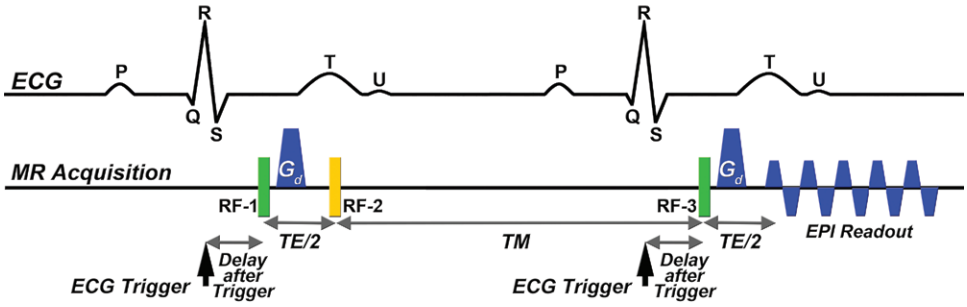

a.

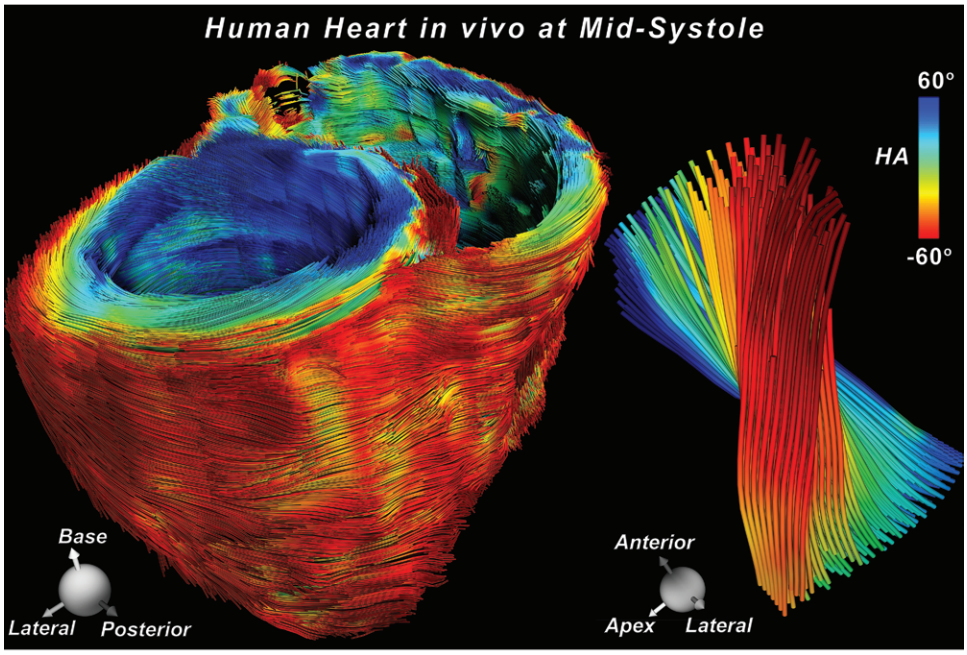

b.

Figure 1: Tractography of the entire human heart in vivo. **(a)** Dual-gated STE sequence. Three 90° excitation pulses *(RF)* are applied over two successive heartbeats. The excitation *(RF-1),* refocusing *(RF-3),* and diffusion dephase and rephase occur at the same time in the R-R intervals, thereby exploiting the periodicity of heart motion to rewind motion-related dephasing. Additionally, the long diffusion time (including mixing time), allows a sufficient *b* value to be produced on clinical imagers without the need for an excessively long echo time *(TE).* **(b)** Tractograms of the heart in a healthy male subject in his mid-30s, acquired with STE. Twelve contiguous short-axis sections were acquired with no SMS excitation during multiple breath holds. Tractograms of the whole heart were generated and color-coded by using myofiber helix angle (HA). A magnified view of fiber tracts intersecting a region of interest in the LV lateral wall exhibits the progression in HA from endocardium to epicardium. *ECG* = electrocardiogram, *EPI* = echo-planar imaging, G_d = diffusion-encoding gradient.

(3,13). SMS excitation was followed by a blipped-CAIPI readout by using a section-phase-section zonal excitation scheme (Fig 1a). For rate 2 SMS excitation, the relative phase axis shift was field of view divided by 3, while rate 3 SMS excitation was field of view divided by 4. Variable-rate selective excitation was used to reduce radiofrequency power (14). For rate 2 SMS excitation, separation between simultaneously excited sections was 48 mm, while separation was 32 mm for rate 3 SMS excitation.

Study Design

Approval of the institutional review board of the hospital and written consent from each study participant were obtained. The study was compliant with the Health Insurance Portability and Accountability Act. The data were

collected in three phases. Phase I involved breath-hold imaging in a cohort of seven healthy volunteers. The entire LV was imaged in its short-axis orientation with no SMS excitation and rate 2 and rate 3 SMS excitation. In phase II, free-breathing DT imaging was performed in the same cohort with no SMS excitation and rate 2 and rate 3 SMS excitation, but rate 3 SMS excitation yielded insufficient image quality. Therefore, during free breathing, the entire LV was imaged by using rate 2 SMS excitation in its short-axis orientation. To further reduce the imaging time, we acquired six contiguous horizontal long-axis (four-chamber view) sections by using rate 2 SMS excitation. Separation between simultaneously excited sections in the four-chamber view was 24 mm. All other acquisition parameters were as indicated earlier. In phase III, patients with pulmonary hypertension underwent imaging by using free-breathing rate 2 SMS excitation.

Sequential Acquisition of Diffusion-encoding Directions

For breath-hold DT imaging, the default interleaved gradient ordering was used (1,3–5,15). In each breath hold, images acquired with a b value of 0 sec/mm^2 were followed by acquisition in 10 diffusion-encoding directions with a b value of 500 sec/mm^2. Eight repetitions, each requiring a breath hold, were performed for magnitude averaging. When free breathing is introduced, some images must be rejected because of periodic displacement from respiration. The default interleaved gradient order tended to distribute these image rejections unevenly across the diffusion directions. In contrast, acquiring the diffusion directions sequentially evenly distributes the rejections across all the diffusion directions and ensures sufficient samples of each diffusion-encoding direction.

Spatiotemporal Registration

Spatiotemporal registration (STR) was developed to reduce the misregistration that resulted from respiratory motion. STR is an automated registration approach based on matching radial intensity profiles over all repetitions. This approach recovers translations and rotations by minimizing the mean square distance between profiles of a reference image obtained with a b value of 0 sec/mm^2 and all other diffusion-weighted images.

Entropy-based Retrospective Image Selection

Respiratory motion during the mixing time causes marked signal cancellation on some of the images. These corrupted images must be rejected to maximize the resulting SNR. After STR, we applied entropy-based retrospective image selection (ERIS) to accept or reject the diffusion-free and diffusion-weighted images. An entropy measure (E_M) based on Shannon's definition of entropy was calculated from the distribution of signal intensity within the myocardium across repetitions (16). Images with E_M within a prescribed range E_R were accepted ($E_M \in E_R$), while those highly affected by artifact were rejected ($E_M \notin E_R$). The acceptance range E_R was independently adjusted for a b value of 0 sec/mm^2 and each diffusion direction.

Image Analysis

Mean diffusivity, fractional anisotropy (FA), and HA were calculated as described previously (17–19). Tractography was performed by numerically integrating the primary eigenvector field into streamlines by using an adaptive 5th-order Runge-Kutta approach (8). Statistical comparison between groups in the study was performed by using a paired t test and analysis of variance. Authors' principal contributions include sequence development (T.G.R., K.S., and H.B.), reconstruction development (S.F.C., K.S., and H.B.), data acquisition (C.M., T.G.R., and D.E.S.), and image processing and analysis (C.M. and M.P.J.). K.S. and colleagues invented the blipped-CAIPI SMS echo-planar imaging technique used in this study, and Massachusetts General Hospital holds the patent. All authors had more than 10 years of experience with MR imaging in these roles.

Results

Breath-hold DT Imaging Acquisition

With no SMS excitation, 96 breath holds (12 sections, eight repetitions) were required to cover the entire LV without section gaps. An example of whole-heart tractography performed during breath hold without section acceleration (ie, no SMS excitation) is shown in Figure 1b. Rate 2 and rate 3 SMS excitation decreased the number of breath holds to 48 and 32, respectively. Only minor qualitative differences between tractograms of the LV with no SMS excitation and rate 2 or rate 3 SMS excitation during breath hold were observed (Fig 2). No significant differences ($P > .69$) were seen in transmural HA, mean diffusivity (mean ± standard deviation, $[0.85 \pm 0.08] \times 10^{-3}$ mm^2/sec, $[0.88 \pm 0.09] \times 10^{-3}$ mm^2/sec, and $[0.89 \pm 0.09] \times 10^{-3}$ mm^2/sec, respectively), or FA (0.41 ± 0.02, 0.42 ± 0.05, and 0.43 ± 0.05, respectively) between no SMS excitation and rate 2 or rate 3 SMS excitation (Fig E1a–1c [online]).

Free-breathing DT Imaging Acquisition

Free-breathing DT images acquired with the sequential gradient order are shown in Figure E2a (online). The eight repetitions at a b value of 0 sec/mm^2 (first column) were acquired sequentially, followed by the eight images in the first diffusion-encoding direction (second column), and so forth. Figure E2b (online) demonstrates how the stepwise addition of STR and ERIS improves the quality of mean diffusivity, FA, and HA maps. For a midventricular section, the entropy measure E_M varied between 6.39 and 7.17, with $E_R \in [0, 6.54]$, which corresponds to the bottom 20% of E_M values.

Comparison between Breath-hold and Free-breathing Acquisitions

Successful tractography of the entire LV was achieved by using both breath-hold rate 3 SMS excitation and free-breathing rate 2 SMS excitation (Fig E3a, 3b [online]). Our accelerated

Figure 2

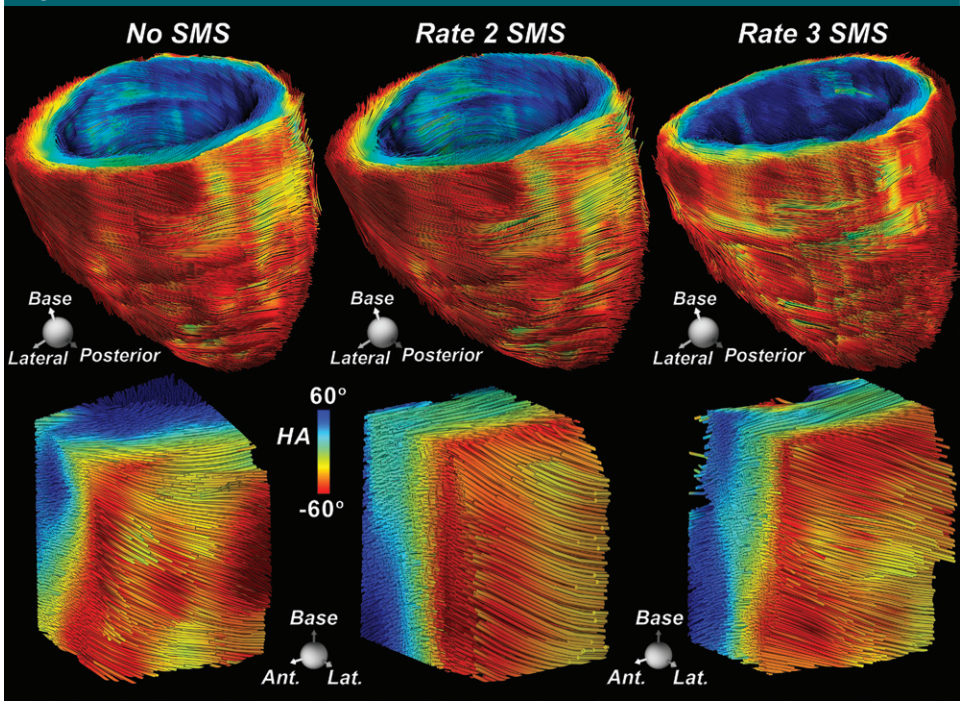

Figure 2: Tractography of the LV performed by using SMS excitation with a blipped-controlled aliasing in parallel imaging readout in a healthy male subject in his mid-30s. Fiber tracts of the entire LV and tracts within a region of interest in the lateral wall were obtained from acquisitions with no SMS excitation, rate 2 SMS excitation, and rate 3 SMS excitation. The tractograms were consistent across all acquisitions. However, the number of breath holds was reduced from 96 with no SMS excitation to 48 and 32 with rate 2 and rate 3 SMS excitation, respectively.

approach combined with STR and ERIS demonstrates the feasibility of producing tractograms by using free-breathing rate 2 SMS excitation, with quality comparable to that obtained with breath-hold rate 3 SMS excitation. No significant differences between breath-hold rate 3 SMS excitation and free-breathing rate 2 SMS excitation ($P > .63$) were seen in HA profiles, mean diffusivity ($[0.89 \pm 0.09] \times 10^{-3}$ mm^2/sec and $[0.9 \pm 0.09] \times 10^{-3}$ mm^2/sec, respectively), or FA (0.43 ± 0.05 and 0.42 ± 0.06, respectively) (Fig E3c [online]).

Comparison between Short-Axis and Four-Chamber Free-breathing Acquisitions

Free-breathing DT imaging with rate 2 SMS excitation was performed successfully for the short-axis and four-chamber views of the heart, producing similar HA maps and tractograms of the LV (Fig E4a [online]). There was no significant difference between short-axis and four-chamber acquisitions ($P > .34$) for HA, mean diffusivity ($[0.9 \pm 0.09] \times 10^{-3}$ mm^2/sec and $[0.89 \pm 0.08] \times 10^{-3}$ mm^2/sec, respectively), or FA (0.42 ± 0.06 and 0.42 ± 0.05, respectively) (Fig E4b–E4d [online]).

Patients with Pulmonary Hypertension

All three patients had advanced pulmonary fibrosis (Fig E5a [online]) complicated by pulmonary hypertension and right ventricular volume overload (Fig E5b [online]). Free-breathing DT imaging with rate 2 SMS excitation was performed successfully in the short-axis and four-chamber views. Myofibers in the subendocardium and midmyocardium of the septum assumed a more rightward orientation (blue), noticeably at the right ventricular insertion points, as shown by means of tractography and the helix angle map (Fig E5c [online]).

Discussion

While cardiac diffusion imaging was first demonstrated in 1994 (20), its clinical translation has been challenging. There has been a renewed interest in this field owing to stronger gradients, multichannel receive coils, dedicated higher-order shimming, and acceleration techniques (12,21,22). In previous studies, multiple breath holds or synchronized breathing (1,3) has been required, with partial anatomic coverage of the LV and comparatively long imaging times (4,5), even with accelerated techniques, such as SMS excitation (11). In this study, we demonstrate a free-breathing DT imaging approach with complete coverage of the human heart in approximately 15 minutes, enabling 3D tractography.

Central to this effort has been our ability to accelerate image acquisition. In-plane acceleration by using

generalized autocalibrating partially parallel acquisition reduces image distortions and shortens the echo time. Through-plane acceleration with SMS excitation is pivotal, reducing acquisition time by the fraction of the SMS excitation rate, with minimal cost in SNR.

Respiratory motion during diffusion encoding can cause complete cancellation of signal in the myocardium. Free-breathing acquisitions mitigate this signal loss with the use of respiratory gating with navigator echoes, or, retrospectively, with the use of postprocessing techniques that eliminate adversely affected images. In this work, we developed a combined approach by using STR and ERIS to align and select the usable images. To ensure that we have sufficient directions and temporal samples, we acquire 10 directions in a sequential order, which yields a fully determined tensor. Advantages of our approach include its fixed acquisition time and the retention of all the acquired data. In contrast, navigator echoes discard data at a run time that could be used for tensor estimation.

Myocardial structure is conventionally characterized by using HA, mean diffusivity, and FA (5,23). No significant differences were found in these indexes when comparing breath-hold rate 3 SMS excitation with free-breathing rate 2 SMS excitation, which produces similar 3D tractograms of the entire LV, although certainty could be improved with larger sample size. Accelerated free-breathing DT imaging of the human heart was also performed in the four-chamber view. This led to a twofold reduction in imaging time and better characterization of the anteroapex and true apical walls. There was no statistical difference in HA, mean diffusivity, or FA between short-axis and four-chamber acquisitions, which yields similar tractograms of the LV.

The ability to image patients with advanced pulmonary fibrosis with the free-breathing approach is encouraging. All patients were using oxygen at home, were being considered for lung transplantation, and had deep and irregular respiratory patterns. After DT imaging acquisition of the entire LV, tractography was performed and exhibited a reorganization of fibers in the septum, with increased rightward rotation at the right ventricular insertion points. Further study in patients with pulmonary hypertension and right ventricular overload will be needed to confirm these preliminary findings.

Recently, motion-compensated pulsed gradient spin-echo imaging (24) and diffusion-prepared balanced steady-state free-precession imaging (25) have demonstrated promising results for in vivo diffusion imaging. However, both sequences are sensitive to respiratory motion and could benefit from our free-breathing, image alignment and retrospective image selection approach. A potential advantage of the motion-compensated pulsed gradient spin-echo approach is a significant reduction of repetition time in comparison to STE imaging, which could result in imaging times of 10 minutes or less, which further removes barriers to clinical translation.

In conclusion, we introduce a clinically feasible, whole-heart, free-breathing accelerated DT imaging approach, with an imaging time of approximately 15 minutes. Imaging the myocardium in the four-chamber view further reduces imaging time and may prove valuable in characterizing remodeling in the anterior and apical walls. These advances may facilitate clinical translation of DT imaging, which enables reliable characterization of myocardial structure in patients with heart failure and other cardiovascular diseases.

Disclosures of Conflicts of Interest: C.M. disclosed no relevant relationships. **T.G.R.** disclosed no relevant relationships. **M.P.J.** disclosed no relevant relationships. **S.F.C.** disclosed no relevant relationships. **K.S.** Activities related to the present article: disclosed no relevant relationships. Activities not related to the present article: author received payment for a U.S. patent for blipped-CAIPI (patent no. 8405395). Other relationships: author and institution received royalties from General Electric and Philips Healthcare. **H.B.** Activities related to the present article: disclosed no relevant relationships. Activities not related to the present article: author is an employee of Siemens Healthcare. Other relationships: disclosed no relevant relationships. **D.E.S.** disclosed no relevant relationships.

References

1. Reese TG, Weisskoff RM, Smith RN, Rosen BR, Dinsmore RE, Wedeen VJ. Imaging myocardial fiber architecture in vivo with magnetic resonance. Magn Reson Med 1995; 34(6):786–791.
2. Gamper U, Boesiger P, Kozerke S. Diffusion imaging of the in vivo heart using spin echoes—considerations on bulk motion sensitivity. Magn Reson Med 2007;57(2):331–337.
3. Tseng WY, Reese TG, Weisskoff RM, Wedeen VJ. Cardiac diffusion tensor MRI in vivo without strain correction. Magn Reson Med 1999;42(2):393–403.
4. Nielles-Vallespin S, Mekkaoui C, Gatehouse P, et al. In vivo diffusion tensor MRI of the human heart: reproducibility of breath-hold and navigator-based approaches. Magn Reson Med 2013;70(2):454–465.
5. Wu MT, Su MY, Huang YL, et al. Sequential changes of myocardial microstructure in patients postmyocardial infarction by diffusion-tensor cardiac MR: correlation with left ventricular structure and function. Circ Cardiovasc Imaging 2009;2(1):32–40, 6, 40.
6. Trayanova NA. Whole-heart modeling: applications to cardiac electrophysiology and electromechanics. Circ Res 2011;108(1): 113–128.
7. Pantoja JL, Ge L, Zhang Z, et al. Posterior papillary muscle anchoring affects remote myofiber stress and pump function: finite element analysis. Ann Thorac Surg 2014;98(4): 1355–1362.
8. Mekkaoui C, Huang S, Chen HH, et al. Fiber architecture in remodeled myocardium revealed with a quantitative diffusion CMR tractography framework and histological validation. J Cardiovasc Magn Reson 2012;14:70.
9. Setsompop K, Gagoski BA, Polimeni JR, Witzel T, Wedeen VJ, Wald LL. Blipped-controlled aliasing in parallel imaging for simultaneous multislice echo planar imaging with reduced g-factor penalty. Magn Reson Med 2012;67(5):1210–1224.
10. Setsompop K, Cohen-Adad J, Gagoski BA, et al. Improving diffusion MRI using simultaneous multi-slice echo planar imaging. Neuroimage 2012;63(1):569–580.
11. Lau AZ, Tunnicliffe EM, Frost R, Koopmans PJ, Tyler DJ, Robson MD. Accelerated human cardiac diffusion tensor imaging using simultaneous multislice imaging. Magn Reson Med 2015;73(3):995–1004.
12. Griswold MA, Jakob PM, Heidemann RM, et al. Generalized autocalibrating partially

parallel acquisitions (GRAPPA). Magn Reson Med 2002;47(6):1202–1210.

13. Stoeck CT, Kalinowska A, von Deuster C, et al. Dual-phase cardiac diffusion tensor imaging with strain correction. PLoS One 2014;9(9):e107159.
14. Hargreaves BA, Cunningham CH, Nishimura DG, Conolly SM. Variable-rate selective excitation for rapid MRI sequences. Magn Reson Med 2004;52(3):590–597.
15. Scott AD, Ferreira PF, Nielles-Vallespin S, et al. Optimal diffusion weighting for in vivo cardiac diffusion tensor imaging. Magn Reson Med 2015;74(2):420–430.
16. Tsai DY, Lee Y, Matsuyama E. Information entropy measure for evaluation of image quality. J Digit Imaging 2008;21(3):338–347.
17. Basser PJ. Inferring microstructural features and the physiological state of tissues from diffusion-weighted images. NMR Biomed 1995;8(7-8):333–344.
18. Pierpaoli C, Basser PJ. Toward a quantitative assessment of diffusion anisotropy. Magn Reson Med 1996;36(6):893–906.
19. Scollan DF, Holmes A, Winslow R, Forder J. Histological validation of myocardial microstructure obtained from diffusion tensor magnetic resonance imaging. Am J Physiol 1998;275(6 Pt 2):H2308–H2318.
20. Edelman RR, Gaa J, Wedeen VJ, et al. In vivo measurement of water diffusion in the human heart. Magn Reson Med 1994;32(3):423–428.
21. Pruessmann KP, Weiger M, Scheidegger MB, Boesiger P. SENSE: sensitivity encoding for fast MRI. Magn Reson Med 1999;42(5):952–962.
22. Schmitt M, Potthast A, Sosnovik DE, et al. A 128-channel receive-only cardiac coil for highly accelerated cardiac MRI at 3 Tesla. Magn Reson Med 2008;59(6):1431–1439.
23. Sosnovik DE, Mekkaoui C, Huang S, et al. Microstructural impact of ischemia and bone marrow-derived cell therapy revealed with diffusion tensor magnetic resonance imaging tractography of the heart in vivo. Circulation 2014;129(17):1731–1741.
24. Stoeck CT, von Deuster C, Genet M, Atkinson D, Kozerke S. Second-order motion-compensated spin echo diffusion tensor imaging of the human heart. Magn Reson Med 2016;75(4):1669–1676.
25. Nguyen C, Fan Z, Sharif B, et al. In vivo three-dimensional high resolution cardiac diffusion-weighted MRI: a motion compensated diffusion-prepared balanced steady-state free precession approach. Magn Reson Med 2014;72(5):1257–1267.